Ocean dynamics and biological feedbacks limit the potential of macroalgae carbon dioxide removal

Manon Berger, Lester Kwiatkowski, David T. Ho, Laurent Bopp

ENVIRONMENTAL RESEARCH
LETTERS

LETTER • OPEN ACCESS

Ocean dynamics and biological feedbacks limit the potential of macroalgae carbon dioxide removal

To cite this article: Manon Berger *et al* 2023 *Environ. Res. Lett.* **18** 024039

IOP Publishing Environ. Res. Lett. 18 (2023) 024039 https://doi.org/10.1088/1748-9326/acb06e

ENVIRONMENTAL RESEARCH
LETTERS

OPEN ACCESS

RECEIVED
17 October 2022

REVISED
23 December 2022

ACCEPTED FOR PUBLICATION
5 January 2023

PUBLISHED
6 February 2023

LETTER

Ocean dynamics and biological feedbacks limit the potential of macroalgae carbon dioxide removal

Manon Berger[1,*], **Lester Kwiatkowski**[2], **David T Ho**[3] and **Laurent Bopp**[1]

[1] LMD/IPSL, Ecole Normale Supérieure/Université PSL, CNRS, Ecole Polytechnique, Sorbonne Université, Paris, France
[2] LOCEAN/IPSL, Sorbonne Université, CNRS, IRD, MNHN, Paris, France
[3] Department of Oceanography, University of Hawai'i at Mānoa, Honolulu, HI, United States of America
[*] Author to whom any correspondence should be addressed.

E-mail: manon.berger@lmd.ipsl.fr

Keywords: carbon dioxide removal, CDR, macroalgae cultivation, air–sea equilibrium, seaweed, kelp, MRV

Supplementary material for this article is available online

Abstract

In combination with drastic emission reduction cuts, limiting global warming below 1.5 °C or 2 °C requires atmospheric carbon dioxide removal (CDR) of up to 16 $GtCO_2$ yr^{-1} by 2050. Among CDR solutions, ocean afforestation through macroalgae cultivation is considered promising due to high rates of productivity and environmental co-benefits. We modify a high-resolution ocean biogeochemical model to simulate the consumption of dissolved inorganic carbon and macronutrients by idealised macroalgal cultivation in Exclusive Economic Zones. Under imposed macroalgal production of 0.5 PgC yr^{-1} with no nutrient feedbacks, physicochemical processes are found to limit the enhancement in the ocean carbon sink to 0.39 PgC yr^{-1} (1.43 $GtCO_2$ yr^{-1}), corresponding to CDR efficiency of 79%. Only 0.22 PgC yr^{-1} (56%) of this air–sea carbon flux occurs in the regions of macroalgae cultivation, posing potential issues for measurement, reporting, and verification. When additional macronutrient limitations and feedbacks are simulated, the realised macroalgal production rate drops to 0.37 PgC yr^{-1} and the enhancement in the air–sea carbon flux to 0.21 PgC yr^{-1} (0.79 GtCO yr^{-1}), or 58% of the macroalgal net production. This decrease in CDR efficiency is a consequence of a deepening in the optimum depth of macroalgal production and a reduction in phytoplankton production due to reduced nitrate and phosphate availability. At regional scales, the decrease of phytoplankton productivity can even cause a net reduction in the oceanic carbon sink. Although additional modelling efforts are required, Eastern boundary upwelling systems and regions of the Northeast Pacific and the Southern Ocean are revealed as potentially promising locations for efficient macroalgae-based CDR. Despite the CDR potential of ocean afforestation, our simulations indicate potential negative impacts on marine food webs with reductions in phytoplankton primary production of up to −40 gC m^{-2} yr^{-1} in the eastern tropical Pacific.

1. Introduction

Limiting global warming to 1.5 °C or 2 °C above preindustrial values will require deep and fast, if not immediate, transitions in all emissions sectors [1]. Even if such emission reduction efforts are implemented, large-scale deployment of carbon dioxide removal (CDR) may be required to meet 1.5 °C or 2 °C targets [2, 3] and to offset greenhouse gas emissions from sectors that cannot fully decarbonise or are likely to require a long time to do so [4–6]. CDR methods are defined as deliberate actions to remove CO_2 directly from the atmosphere and durably store it in geological, terrestrial, or ocean reservoirs. As discussed in the recent IPCC 6th Assessment Report, many of the scenarios likely to limit warming to 2 °C or below require CDR, up to 16 $GtCO_2$ yr^{-1} by 2050 [7, 8].

The ocean offers many potential opportunities for enhanced mitigation [9, 10]. Proposals typically focus on either enhancing biological ocean carbon sinks through marine afforestation and

fertilisation or chemically increasing the inorganic ocean carbon sink through techniques such as ocean alkalinity enhancement [11]. Among ocean-based CDR approaches, large-scale ocean afforestation by macroalgae has received growing interest [12–14]. Macroalgae can support photosynthetic productivity comparable to that of a tropical rainforest [15, 16] with a high carbon content [17], making them potential candidates for ocean-based CDR. Moreover, they do not compete with agricultural land and may provide local benefits such as reduced eutrophication [18] and acidification [19]. Several post-growth pathways for harvested macroalgae biomass have been proposed, including the production of long-lived bio-products or facilitating the transport of biomass into the deep ocean. However, there are concerns about the adverse impact of macroalgae afforestation on natural ecosystems [20, 21].

Evaluating macroalgal carbon sequestration potential is more complex than with terrestrial analogues [22–25]. Because macroalgae do not fix carbon directly from the atmosphere but from the ocean, assessing macroalgal-based CDR potential requires consideration of ocean–atmosphere CO_2 exchange, and thus ocean circulation and mixing, carbonate chemistry, as well as interactions with other biological carbon sinks and sources [22]. Studies that have evaluated the global CDR potential of macroalgal cultivation have generally upscaled observed growth rates of some macroalgal species to the global ocean [14, 26]. Global dynamic models of macroalgae cultivation have begun to be developed, simulating the growth of macroalgae [27], and refining estimates of the carbon sequestration potential of global macroalgal cultivation from 3.7 $GtCO_2\ yr^{-1}$ [28] to 13.3 $GtCO_2\ yr^{-1}$ [29]. Using the Sargassum Belt as a natural analogue for ocean afforestation, biochemical feedbacks (i.e. the effects of macroalgal cultivation on remaining ocean nutrient concentrations and subsequent impacts on phytoplankton) have been shown to reduce the CDR potential of macroalgae by 20%–100% [30]. However, all studies to date either omit certain geochemical and biological feedbacks [27, 28, 30] or use global-scale coarse resolution models [29]. As such, there are currently poor constraints on the efficiency of large-scale macroalgae-based CDR, its environmental co-benefits and consequences, and the potential optimum regions for deployment [31].

Here, we perform simulations using a high-resolution ocean biogeochemical model to assess the efficiency, nutrient feedbacks, and acidification co-benefits of idealised macroalgae-based CDR. Following Froelich *et al*, we limited the macroalgal cultivated zone to Exclusive Economic Zones (EEZs) for reasons of cost limitation and political feasibility [14]. Imposing uniform and unconstrained macroalgal dissolved inorganic carbon (DIC) consumption in the upper 100 m of EEZ regions, we assess the extent to which local-to-global air–sea carbon fluxes are enhanced under present climate conditions. Applying additional macronutrient (nitrate and phosphate) constraints on macroalgae production and assuming that nutrients consumed by macroalgae are permanently removed from the ocean, we assess the decrease in realised macroalgal production and the impact on CDR. Finally, we evaluate how macroalgal carbon and nutrient consumption may influence phytoplankton primary production and coincident ocean acidification.

2. Material and methods

2.1. Ocean-biogeochemical model

Idealised macroalgae CDR simulations were performed with version 3.6 of the ocean modelling framework *Nucleus for European Modelling of the Ocean* (NEMO). This framework includes version 3 of the Louvain-La-Neuve sea Ice Model [32] and version 2 of the *Pelagic Interaction Scheme for Carbon and Ecosystem Studies* (PISCES) biogeochemical model [33]. The model was used with an eddy-permitting ORCA025 configuration [34] with a nominal horizontal resolution of 25 km, enabling adequate representation of EEZ boundaries while simulating the global ocean. The configuration includes 75 vertical depth levels, 23 of which are in the upper 100 m of the water column, where macroalgae growth is considered feasible. The surface ocean layer, which exchanges carbon directly with the atmosphere, is 1 m deep.

PISCES [33] simulates the cycles of essential elements for this study, including carbon (dissolved and particulate organic and inorganic forms), total alkalinity, N, P, Si and Fe. It includes two phytoplankton types (nanophytoplankton and diatoms) and two zooplankton size classes (micro- and mesozooplankton) with a fixed C:N:P stoichiometry of 122:16:1. Phytoplankton production is the product of growth rates and biomass, with growth rates determined based on temperature, light, and nutrient (N, P, Fe, and Si) availability; additionally, biomass is affected by zooplankton grazing. Alongside the living compartments, PISCES simulates semi-labile dissolved organic matter (DOM), formed from phytoplankton and zooplankton particulate organic matter. The remineralization of DOM occurs within the water column and is oxygen-dependent. In addition to implicit diazotrophy, the model considers two external sources of nutrients: river input (NH_4^+, NO_3^-, P, Fe, and Si) and atmospheric deposition (N, P, Fe, and Si). The CO_2 flux at the air–sea interface is determined by the difference in CO_2 partial pressure between the atmosphere and the ocean, the gas transfer velocity (function of the 10 m wind speed and the Schmidt number, which is a function of seawater temperature and salinity), and the solubility of CO_2 in seawater.

The model control simulation was initialized from data-based climatologies and a coarser resolution NEMO-PISCES historical simulation of the anthropogenic ocean carbon inventory [35]. The model is then run from 1958 to 2016 using atmospheric forcings (Drakkar forcing set 5.2 [36]). Historical atmospheric concentrations of CO_2 are annually prescribed.

2.2. Macroalgae simulations

Idealised macroalgal simulations are run over five years (2006–2010) under the same atmospheric forcing as the control run. Macroalgal production occurs within a fixed spatial distribution based on EEZs (corresponding to 20% of the total ocean surface). Simulated macroalgal production is represented as the consumption of DIC, analogous to typical macroalgae, which actively take up seawater HCO_3^- and/or CO_2 for photosynthesis [37]. Maximum global net production is prescribed as 0.5 PgC yr^{-1} (1.8 $GtCO_2$ yr^{-1}), corresponding to about 10% of maximum CDR requirements in 2050 to achieve <2 °C warming [7]. Though this global macroalgal production is lower than previous studies (from 3.7 $GtCO_2$ yr^{-1} [22, 28] to 13.3 $GtCO_2$ yr^{-1} [29]) and is only applied in EEZs, this value remains extremely ambitious and represents about 340 times the cultivated seaweed production in 2019 [38]. The spatial distribution of macroalgae production was restricted to waters of EEZs, in regions free of seasonal sea ice, with a mean sea surface temperature between 0 °C and 35 °C [39] and an average N:P ratio between 4:1 and 80:1 in the upper 100 m. The typical N:P range for macroalgae extends from 10:1 to 80:1 [40], but the lower limit of 4:1 is used to capture areas with known native macroalgae, as in Froelich *et al* [14]. Above 100 m, macroalgal production is unconstrained or limited only by nutrients. Below 100 m, production is assumed to be entirely light-limited. In total, this represents an area of 73 million km^2, with a macroalgal production rate of 6.72 gC m^{-2} yr^{-1}, identical in all grid cells and occurring at every model time step when production is permissible. A global production rate ten times higher (globally 5 PgC yr^{-1}), was also used to test the scalability of our results (see supplementary materials (SOM)).

Given a typical macroalgae carbon content of 29.8% dry weight (DW) [41–48], a DW to wet weight (WW) ratio of 14.34% [45–47], and the defined area of 73 million km^2, macroalgae production of 0.5 PgC yr^{-1} is equivalent to a net growth rate of 0.42 gWW m^{-2} d^{-1}. This is also equivalent to 42 gWW m^{-2} d^{-1} distributed homogeneously in 1% of the EEZ cultivation area, which is in the range of growth rates for *Saccharina latissima, Laminaria digitata* and *Macrocystis pyrifera* [17, 41, 49].

Two idealised global macroalgal simulations were performed, (a) hereafter referred to as 'Geo', where the macroalgal production rate (i.e. DIC consumption) is imposed and independent of changing physical and biogeochemical conditions, and (b) hereafter referred to as 'BioGeo', where the macroalgal production rate is identical to Geo but in addition to DIC, NO_3^- and PO_4^{3-} are taken up by macroalgae at a fixed C:N:P ratio of 800:49:1 [50] and production only occurs if NO_3^- and PO_4^{3-} are sufficient (table 1). It should be noted that simulated macroalgae production in Geo is therefore more nutrient efficient than phytoplankton production, which occurs at a fixed C:N:P stoichiometry of 122:16:1 in PISCES [51]. Differences between the Geo and BioGeo simulations reflect nutrient constraints on macroalgal production and biogeochemical feedbacks. Although both simulations resolve the planktonic community and its impact on carbon export and air–sea fluxes, macroalgae and phytoplankton production are effectively independent in the Geo simulation (figure 1). In the BioGeo simulation, however, macroalgae nutrient consumption can impact phytoplankton production, with consequences for zooplankton grazing, organic matter production and export, and air–sea carbon fluxes. The absence of macroalgal nutrient limitation in Geo can be alternatively interpreted as an artificial supply of all required nutrients with no net carbon emissions associated with this fertilization. All macroalgae production is considered immediately harvested and permanently sequestered with no associated carbon emissions. As such, there is no remineralization of macroalgal biomass. Our simulations therefore likely represent an upper bound on macroalgae CDR potential.

Table 1. Macroalgae simulation names, descriptions and the limitations on macroalgae CDR potential that they assess.

Simulation	Macroalgae tracer consumption	Global macroalgal production rate	Limitations on CDR potential
Geo	DIC	0.5 PgC yr^{-1}, non-limited	Physical and geochemical
BioGeo	DIC, NO_3^-, PO_4^{3-}	0.37 PgC yr^{-1}, nutrient-limited	Physical, geochemical, macrolagae constraints, phytoplankton feedbacks

The global macroalgal production rate in BioGeo is estimated, by considering a closed carbon budget. The total DIC change compared to the control simulation (ΔDIC) is then a combination of the total carbon removed by macroalgal production (C_{ma}) and the change in the total carbon exchange with the atmosphere compared to the control simulation ($\Delta C_{gas,ex}$): $C_{ma} = \Delta DIC - \Delta C_{gas,ex}$.

2.3. Carbon dioxide removal (CDR) efficiency

We define CDR efficiency as the simulated increase in the air–sea carbon flux relative to the

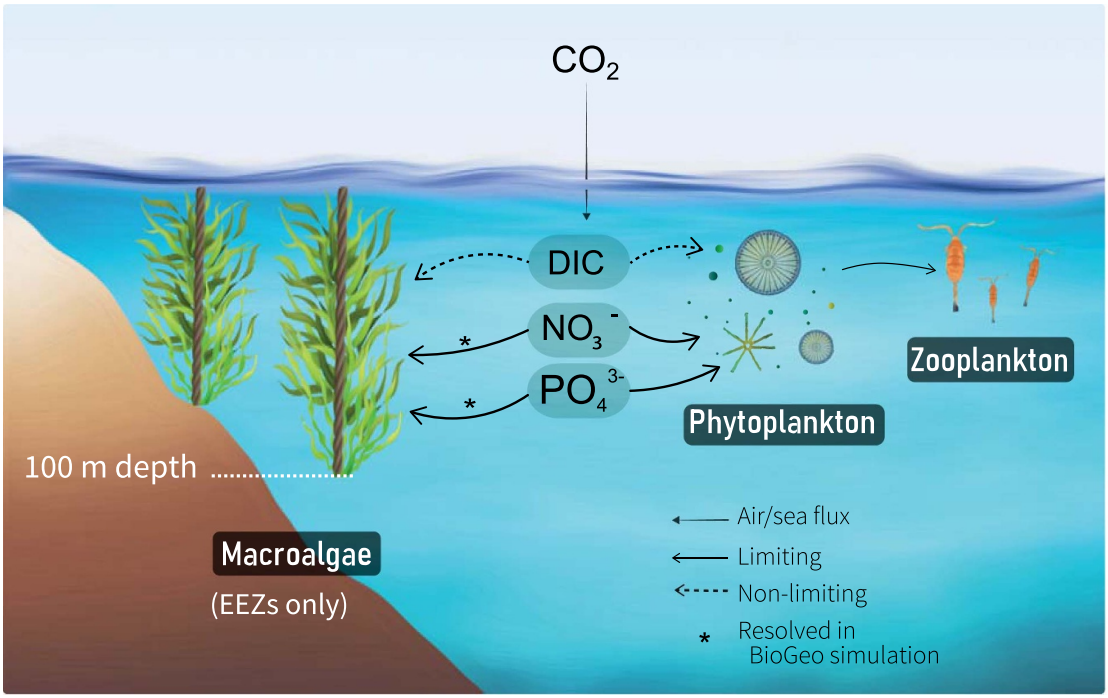

Figure 1. Interactions resolved in the NEMO-PISCES macroalgae simulations. The Geo and BioGeo simulations both resolve macroalgae DIC consumption, air sea carbon fluxes, and the planktonic food web. However BioGeo additionally resolves nitrate and phosphate limitation on macrolgae production, the macroalgal consumption of these nutrients, and the resulting impact on phytoplankton productivity.

maximum attainable macroalgae carbon production given unlimited nutrients (i.e. 0.5 PgC yr^{-1} or 1.8 $GtCO_2$ yr^{-1}). Thus, 100% efficiency implies that the maximal macroalgae carbon production is entirely replaced by the invasion of an equivalent amount of atmospheric carbon. The CDR efficiency is thus a combination of the realised macroalgal production, phytoplankton feedbacks, and the air–sea carbon equilibration. Locally, the CDR efficiency is computed with the mean change in air–sea carbon flux relative to maximum attainable macroalgae production (6.72 gC m^{-2} yr^{-1}). As with the rest of the results, we show the CDR efficiency averaged over 2010, the last year of the simulation. This has the downside of presenting some internal variability but has the upside of eliminating most of the transient regime, with the CDR carbon flux approaching its optimal value. Mean CDR efficiency values over the simulation duration are provided in the SOM.

3. Results

3.1. Global macroalgal CDR efficiency

In the Geo simulation with an imposed macroalgal production of 0.5 PgC yr^{-1}, the increase in ocean carbon uptake from the atmosphere or CDR flux is 0.39 PgC yr^{-1} (1.43 $GtCO_2$ yr^{-1}) on average in 2010 (figure 2). Physical and geochemical processes, therefore, limit the CDR efficiency to 79%, with 21% of the carbon deficit induced by macroalgal production not restored by an invasion of atmospheric carbon on the timescale of our simulations. Only 56% (0.22 PgC yr^{-1}) of the total CDR flux (i.e. the additional air–sea carbon flux) occurs in the regions where macroalgae cultivation is applied, with the rest occurring outside these regions.

In the BioGeo simulation, the CDR flux drops to 0.21 PgC yr^{-1} (0.77 $GtCO_2$ yr^{-1}) due to phytoplankton feedbacks and macroalgal nutrient constraints (figure 2). This corresponds to a global CDR efficiency of 43%, relative to the maximum attainable macroalgae production (0.5 PgC yr^{-1}), or to an invasion of atmospheric carbon balancing 58% of estimated realised macroalgal production. Similar to the Geo simulation, only 52% (0.11 PgC yr^{-1}) of the CDR flux occurs in the area of macroalgae cultivation, with the rest occurring elsewhere. With an imposed macroalgae production rate ten times higher (5 PgC yr^{-1}, see SOM), global CDR efficiencies are found to be similar.

3.2. Regional disparities in macroalgal CDR

In the Geo simulation, the local CDR flux varies from 0.5 to 5.8 gC m^{-2} yr^{-1} (figure 3(a)), even though we imposed homogenous macroalgal production of 6.72 gC m^{-2} yr^{-1}. Similarly, macroalgal CDR efficiency varies from 5% to 85% (figure 4(a)). The lowest CDR fluxes of 0.5–2 gC m^{-2} yr^{-1} are found in the tropics and sub-tropics. These regions also had the lowest CDR efficiencies, ranging from 10% to 25%. Higher CDR fluxes of 2–5.5 gC m^{-2} yr^{-1} and higher

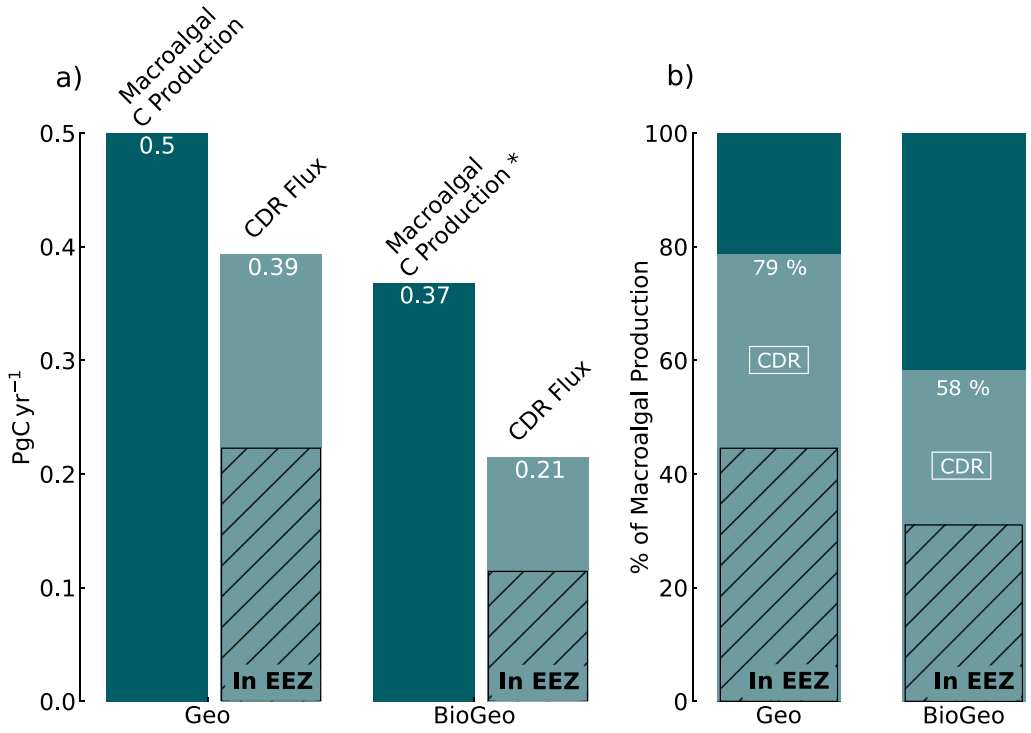

Figure 2. Global macroalgal production and the associated increase in the air–sea carbon flux (CDR) in the Geo and BioGeo simulations. (a) Absolute values of macroalgal production and the enhancement in air–sea carbon flux. (b) CDR flux as a fraction of realised macroalgal production. Hatched areas indicate the CDR flux that occurs within the EEZ cultivation area. Values are for the final simulation year (2010). (*) the realised macroalgal carbon production is estimated in the BioGeo simulation but imposed in the Geo simulation.

CDR efficiencies, from 50% to 75%, are observed in upwelling systems, eastern boundary currents, the South Java Current, the South China Sea, and the higher latitudes. The North Pacific shows the highest flux of 5.8 gC m^{-2} yr^{-1} and the highest efficiency (up to 85%).

In the BioGeo simulation, local CDR fluxes range from −1 to 5.8 gC m^2 yr^{-1} (figure 3(b)) and CDR efficiencies from −14% to 85% (figure 4(b)), with certain areas showing a reduction in the air–sea carbon flux compared to the control simulation. The North Pacific, the Southern Ocean, and upwelling areas show about the same air–sea carbon flux and CDR efficiency as in the Geo simulation. In contrast, lower CDR flux and efficiency is observed in the Indian Ocean, equatorial western Pacific and Atlantic, Canary Current, and Cape Verde Basin. A reduction in ocean carbon uptake from the atmosphere of up to −1 gC m^2 yr^{-1} is induced by macroalgal cultivation in the South Java Current, in the South Philippine Sea (−0.75 gC m^2 yr^{-1}), and in the Caribbean Sea, Ascension Island, and the Mozambique Channel (−0.2 to −0.6 gC m^2 yr^{-1}). These reductions in oceanic carbon uptake result in negative CDR efficiencies ranging from −5% to −14%. Large reductions in CDR efficiency in the BioGeo simulations occur in the tropics and sub-tropical western oceans, where the mean CDR efficiency is globally reduced by 26%. The greatest reductions, however, occur in the South China Sea, the South Java Current, the Mozambique Channel and, the Canary Islands, where CDR efficiency declines by 50%–80% (figure 4(c)).

3.3. Macroalgae nutrient feedbacks affect ocean DIC profiles

At the local scale, macroalgae nutrient limitation, consumption, and reallocation feedbacks (the difference between BioGeo and Geo) can (a) not change the CDR flux (10% of the total cultivation area), (b) decrease the CDR flux (73% of the area) or (c) reverse the air–sea carbon flux and cause a net release of CO_2 to the atmosphere compared to the control simulation (17% of the area) (figure 5(a)). Macroalgae nutrient limitation, consumption and feedbacks do not impact the air–sea carbon flux in upwelling systems, the North Atlantic and Pacific, and the Southern Ocean. Those areas demonstrate no difference between Geo and BioGeo in the DIC vertical profile (figure 5(d)). However, more often, we observe a decrease in the CDR flux. In these areas, there is still a mean decrease in surface DIC concentration in the BioGeo simulation (−0.5 mmol m^{-3}), but it is less pronounced than in the Geo simulation (−3.2 mmol m^{-3}), with the greatest decreases in DIC occurring in the subsurface at around 80 m (figure 5(c)). There is an increase in surface DIC concentration (1.9 mmol m^{-3}) compared to the control in the cultivation areas where the representation

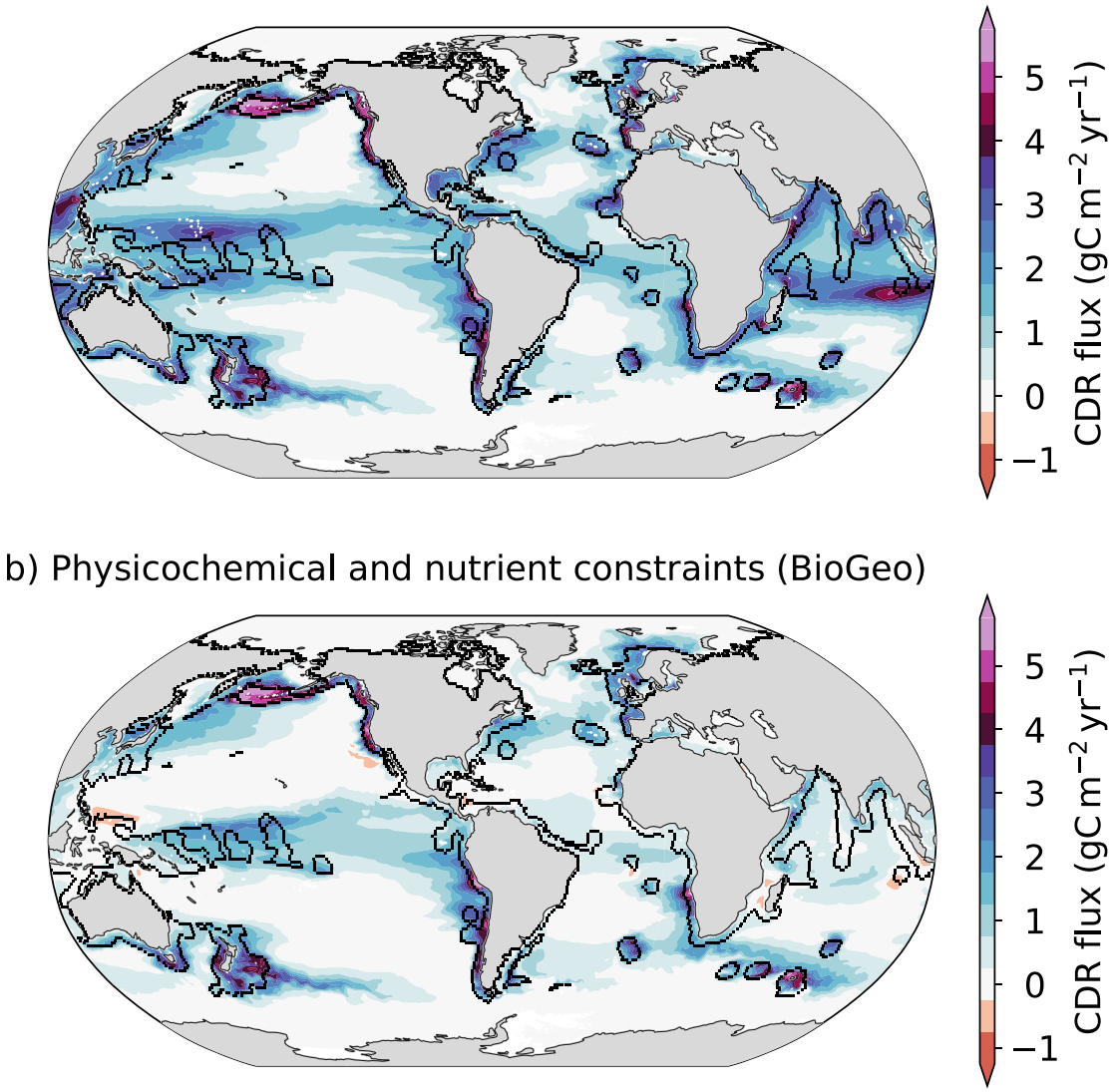

Figure 3. The change in air–sea carbon flux in the (a) Geo and (b) BioGeo simulations (gC m^{-2} yr^{-1}) relative to the control. Values are for the final simulation year (2010). The EEZ macroalgae cultivation boundaries are shown as dotted lines.

of nutrient dynamics in the BioGeo simulation results in outgassing, with the maximum decrease in DIC occurring at around 110 m (figure 5(b)).

3.4. Impact on ocean acidification and phytoplankton primary production

The impact of macroalgae production on ocean acidification and phytoplankton primary production was assessed using the BioGeo simulation that accounts for macroalgae nutrient limitation, consumption, and reallocation feedbacks. Macroalgae production counterbalances ocean acidification, reducing the partial pressure of CO_2 (pCO_2) and increasing pH and the aragonite saturation state. We observe the greatest increase in pH of 0.014 after 5 years in the Southern California Current (figure 6(a)). Our analysis shows an increase of 0.005 per decade in pH in EEZs, while the coincident ocean acidification is about −0.015 per decade in the control. Macroalgae production increases the aragonite saturation state in EEZs by 0.006 per decade (in the control, the same regions exhibit a decline of −0.02 per decade), and the greatest increase of 0.04 is observed in the Eastern American and African upwelling systems (figure 6(c)). A decrease in the aragonite saturation state is observed where pCO_2 increases, in the South Philippine Sea (figure 6(b)).

Macroalgae nutrient consumption reduces depth-integrated net phytoplankton primary production by −3.0 gC m^{-2} yr^{-1} globally and −7.3 gC m^{-2} yr^{-1} on average in EEZs (figure 6(d)). The decrease in the phytoplankton primary production is greatest in the eastern tropical Pacific, where it reaches −37 gC m^{-2} yr^{-1} inside the cultivation area, while it is −42 gC m^{-2} yr^{-1} outside cultivation zones.

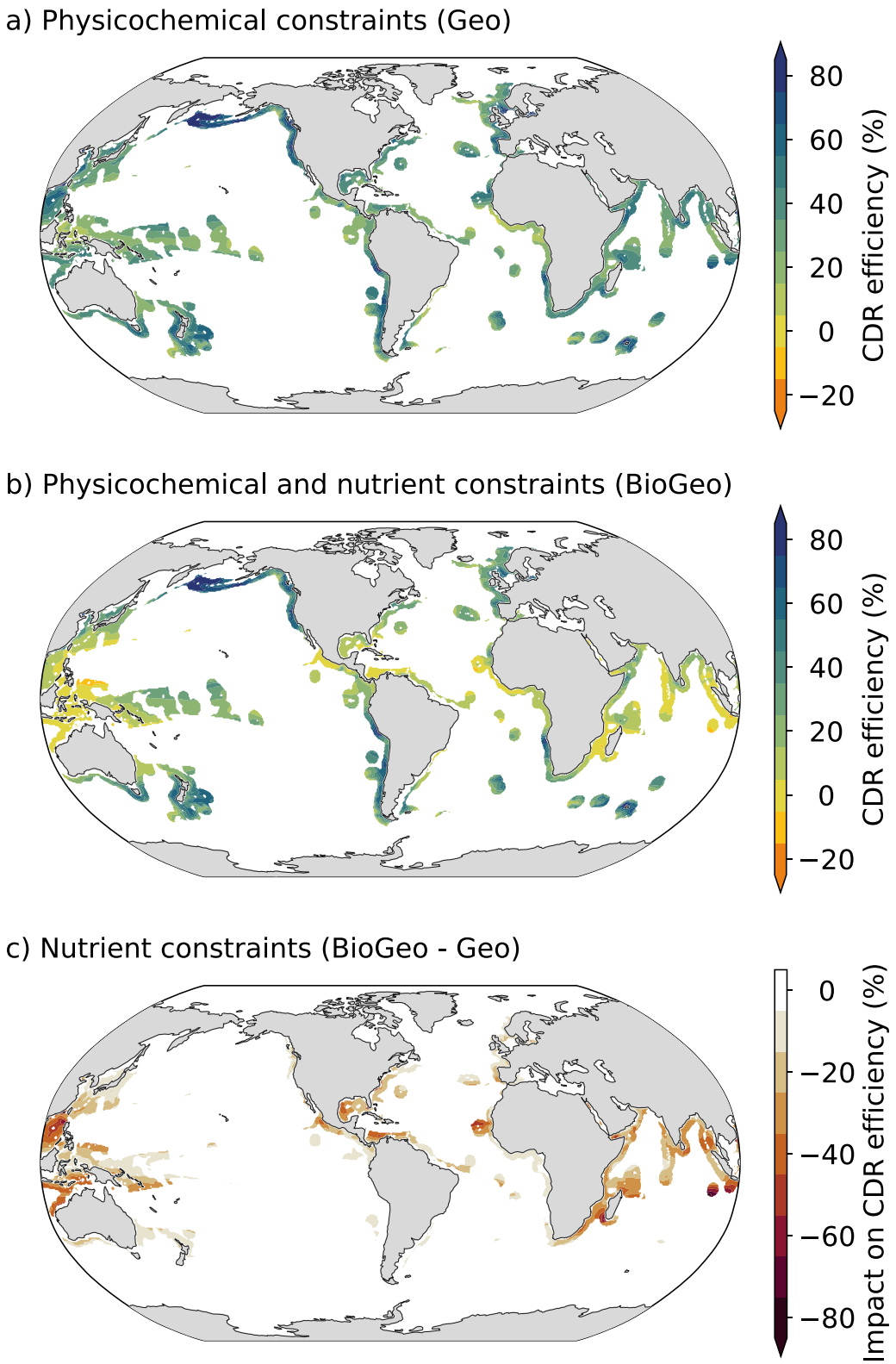

Figure 4. Carbon dioxide removal (CDR) efficiency (%) in the (a) Geo and (b) BioGeo simulations in 2010. (c) The difference in CDR efficiency between Geo and BioGeo is due to macroalgae nutrient limitation and phytoplankton feedbacks.

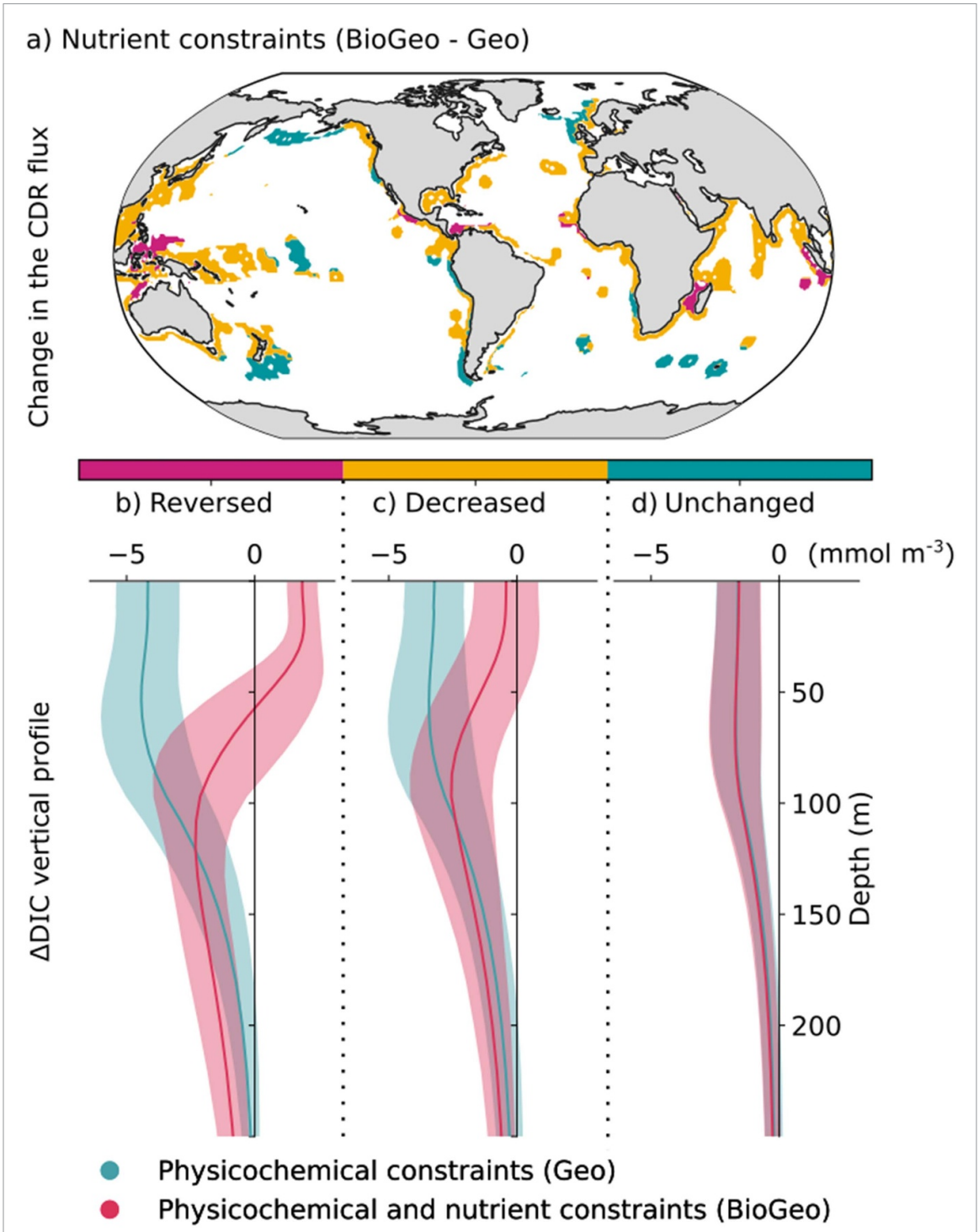

Figure 5. The impact of macroalgae nutrient limitation, consumption and feedbacks on (a) the mean CDR flux (BioGeo–Geo) and the change in DIC vertical profiles in the Geo and BioGeo simulations compared to the control, in areas where the air–sea flux is (b) reversed, (c) decreased, and (d) unchanged. Errors are the spatial standard deviation. Values are for the final simulation year (2010).

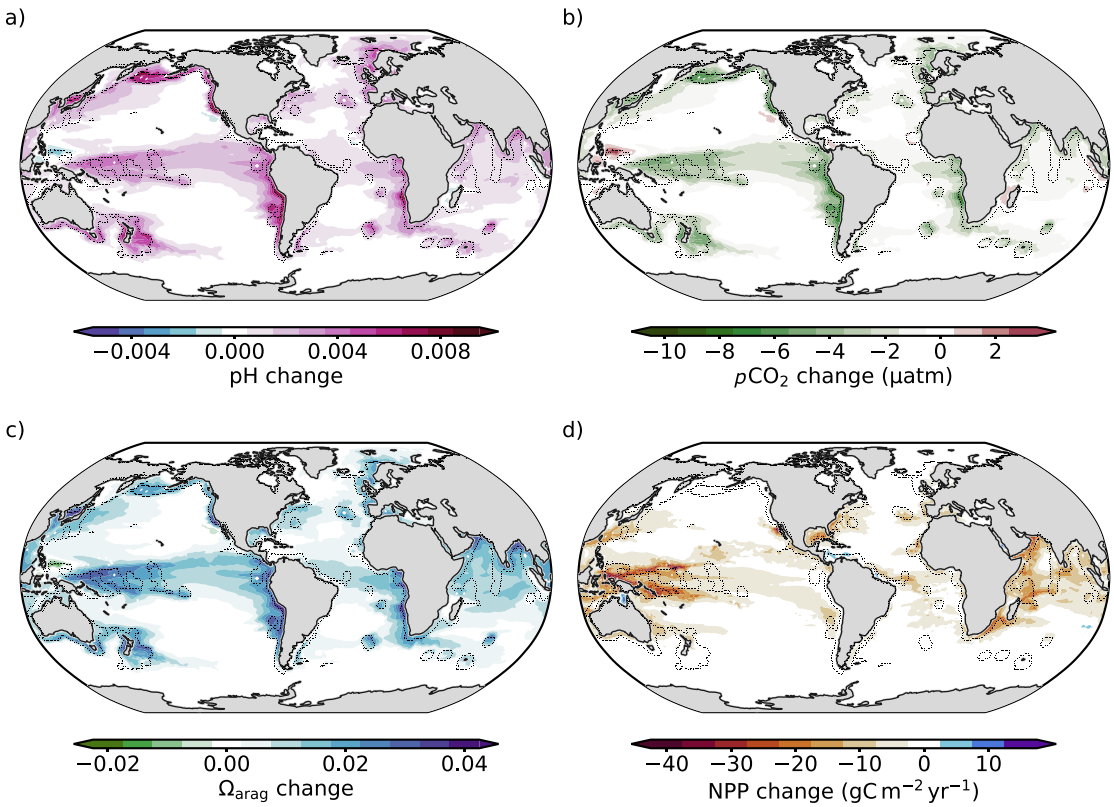

Figure 6. Change in the mean surface ocean (a) pH, (b) pCO_2, (c) aragonite saturation state and (d) the depth-integrated phytoplankton NPP, in the BioGeo simulation relative to the control. Values are for the final simulation year (2010). The EEZ macroalgae cultivation boundaries are shown as dotted lines.

4. Discussion

4.1. Macroalgal CDR efficiency

We modify an ocean biogeochemical model that couples ocean dynamics, air–sea gas exchange, carbonate chemistry, and plankton biology to assess macroalgal CDR efficiency with unprecedented resolution for the level of simulated process complexity. Our analysis shows that physical and geochemical processes limit the present-day global enhancement of the ocean carbon flux to 79% of the macroalgae DIC removal rate (Geo simulation). This 79% CDR efficiency is in broad agreement with previous studies that have used a diversity of models, under different atmospheric conditions and made different macroalgae growth assumptions. For example, a prescribed DIC removal rate of 1 PgC yr^{-1} in the upper 200 m of the tropical and subtropical oceans has been shown to result in a mean CDR efficiency of 72% over 100 years [22]. Accounting for the impact of macroalgae nutrient reallocation on phytoplankton growth further reduces CDR efficiency by 21% (BioGeo simulation). This is within the 7%–50% nutrient reallocation reduction range previously estimated using the Sargassum Belt [30]. A previous modelling study that accounts for macroalgal feedbacks on phytoplankton growth estimated the global macroalgae CDR efficiency to be 75% on multi-centennial timescales [29].

It has been two decades since it was first shown that upper ocean DIC deficits induced by simulated macroalgae production do not fully equilibrate with the atmosphere due to constraints on air–sea gas exchange [22, 25]. The longer timescale of the air–sea equilibrium compared to the residence time of surface seawater [52] allows some of the carbon deficit to be transported to depth before equilibrating with the atmosphere. In our simulations 48% of the global macroalgae-induced DIC deficit is present below the 100 m depth horizon of macroalgae production in the Geo simulation (figure 5). This increases to 82% in the BioGeo simulation, where nutrient limitation deepens the optimum depth of macroalgal production and planktonic feedbacks reduce the export of organic carbon and subsequent remineralization at depth (see SOM).

4.1.1 Physicochemical constraints

In addition to quantifying global CDR efficiency, we find that local CDR efficiencies can vary from 5% to 85% due to physicochemical processes alone. Variable local CDR efficiencies are attributable to a number of physicochemical processes acting on the air–sea carbon flux in a grid cell. Using a multiple linear regression framework, we tested the extent to which spatial variance in local CDR efficiency could be explained by surface ocean CO_2 solubility, Revelle factor, vertical and horizontal advection

in the upper 100 m, seawater age since surface contact in the upper 100 m, and wind speed at 10 m. To prevent collinearity issues, variable selection was performed with recursive feature elimination with cross-validation. The optimal variables selected were the CO_2 solubility and Revelle factor in the surface ocean, and horizontal advection in the upper 100 m.

4.1.1.a CO_2 solubility

Air–sea carbon fluxes are affected by CO_2 solubility [53–55]. In the Geo simulation, we find a positive relationship between the local CO_2 solubility of surface waters and the air–sea carbon uptake induced by macroalgal production ($P < 0.001$, see SOM). This likely explains why warmer tropical waters, with lower CO_2 solubility, typically exhibit lower CDR efficiency than other regions in the Geo simulation.

4.1.1.b Seawater buffering capacity

As we simulate macroalgal production as a loss of DIC from the water column, the associated change in pCO_2 is affected by seawater buffering capacity. Other factors being equal, at lower buffer capacities (i.e. higher Revelle factor), a given decrease in DIC results in a greater decrease in the aqueous CO_2 concentration, a greater decrease in seawater pCO_2 and therefore a greater enhancement in the air–sea CO_2 flux [56]. In agreement with this, we find a positive relationship between the local Revelle factor of surface waters and the air–sea carbon uptake induced by macroalgal production ($P < 0.001$, see SOM). This is likely to at least partially explain why the low buffer capacity waters of the North Pacific exhibit such high CDR efficiencies (>60% in the Geo simulation).

4.1.1.c Horizontal advection

CDR fluxes are influenced by how long a water parcel with a macroalgae-induced carbon deficit is in contact with the atmosphere. Other factors being equal, longer surface residence times result in higher CDR until full equilibration. Transport and mixing of water masses reduce the residence time of macroalgae-induced pCO_2 gradients, limiting CDR. After accounting for CO_2 solubility and the Revelle factor of surface waters, the horizontal advection velocity averaged over the upper 100 m of the water column is found to explain additional variance in local CDR efficiency, with lower CDR in regions of higher horizontal transport ($P < 0.001$, see SOM). This potentially explains why southern Chile, which has high horizontal current velocities associated with the Antarctic Circumpolar Current, has lower CDR efficiency than northern Chile, where horizontal current velocities are lower. As local CDR efficiency is the ratio between maximum potential macroalgae production and the enhancement in air–sea carbon flux at the grid cell level, it does not account for any influence of production on the downstream CDR flux and is therefore sensitive to horizontal advection. Vertical advection also reduces the residence time of macroalgae-induced pCO_2 gradients; however, it was not statistically significant in this study.

4.1.2 Nutrient constraints

In addition to the aforementioned physicochemical processes, CDR efficiency is also modified by macroalgae nutrient limitation and competition between macroalgae and phytoplankton for nutrients, as shown by local differences in Geo and BioGeo CDR efficiencies (figure 4(c)). Much of the surface ocean has insufficient nutrient concentrations to sustain the prescribed macroalgae production rate of the Geo simulation in the BioGeo simulation. This acts to shift maximum macroalgae production and consumption, of DIC to the subsurface (figure 5), with reduced impact on the air–sea pCO_2 gradient and less efficient CDR. The magnitude of this reduction in CDR efficiency depends on the initial surface ocean macronutrient concentrations and the turnover time of depleted nutrients. As such, in contrast to most of the tropics and subtropics, nutrient-replete high-latitude regions and upwelling systems can demonstrate no reduction in CDR efficiencies from the Geo to BioGeo simulation. The consumption of nutrients by macroalgae can further influence local CDR efficiencies by reducing phytoplankton primary production. In a region where phytoplankton production is N or P limited, the consumption of nutrients by macroalgae, either locally or in waters that are transported into the region, will reduce phytoplankton production. Depending on the relative local magnitude of macroalgae production and the reduction of phytoplankton production, as well as their vertical distribution within the water column, this can enhance surface ocean DIC concentrations and reduce the local ocean carbon sink relative to the control, as seen in the West Pacific. Although more realistic modelling efforts are required, our analysis highlights Eastern boundary upwelling systems and regions of the Northeast Pacific and the Southern Ocean as potentially promising regions for efficient macroalgae-based CDR with limited phytoplankton feedbacks.

4.2. Measurement, reporting, and verification (MRV) challenges

MRV for ocean CDR is a multi-step framework via which carbon credits can be issued and certified and will be essential to the financing of any CDR method. Conventional MRV for macroalgae cultivation would require the amount of macroalgae induced CDR to be measured over a given time period relative to historical control measurements.

Oceanic transport carries waters out of the EEZ cultivation area before they are fully re-equilibrated with the atmosphere. Thus, half of the total CDR flux occurs outside the macroalgal cultivation areas (figure 2), highlighting obvious challenges associated

with assigning carbon credits. It also highlights the extensive spatial scales over which accurate MRV of macroalgae CDR will be required. In addition to the spatial extent of monitoring, quantifying CDR from changes in the ocean CO_2 system is likely to be challenging due to relatively high natural variability, particularly in the more dynamic coastal ocean regions that are more favourable for deployment. Our simulations further highlight how ocean circulation may limit the attribution of a DIC deficit (or enhanced air–sea carbon flux) to a specific macroalgal afforestation project. MRV of macroalgae-based CDR is therefore likely to rely on the use of tracers of water mass residence time, ocean circulation, and gas exchange coupled with calibrated and validated numerical simulations.

4.3. Caveats

While our idealized simulations highlight biogeophysical limits on macroalgae CDR potential, multiple factors with the capacity to influence our results are either unaddressed within our model framework or could be further refined. Longer simulations of our high-resolution ocean biogeochemical model are constrained by its computational cost but are likely to influence our results. Indeed, the macroalgal-induced air–sea carbon flux increases over our 5 year simulations and has not stabilized by the final year. Nonetheless our finding of CDR efficiencies substantially below 100% is in agreement with longer simulations of lower resolution models [22, 29].

Although a sensible initial approach, our representation of macroalgae growth as vertically uniform DIC consumption in the upper 100 m of the water column, where nitrate, phosphate and light are non-limiting, is unrealistic. Explicit representation of macroalgae, where growth rates are time varying and dependent on temperature, light and nutrient availability has the potential to influence our estimates of CDR efficiency. Refinement of the biological realism of simulations should further consider multiple macroalgae species with distinct life history traits and representation of macroalgae canopy shading and direct macroalgae-phytoplankton nutrient competition [57]. Post-growth pathways of macroalgal organic carbon should also be explicitly considered. Our assumption that macroalgae is harvested at no carbon cost is clearly unrealistic, and if macroalgae carbon is to be sequestered *in situ* through some form of transport to the deep ocean then potential remineralization pathways should be represented.

Finally, our use of an ocean biogeochemical model forced by near surface atmospheric fields including prescribed CO_2 concentrations neglects potential feedbacks within the Earth system which could further limit macroalgal CDR potential. Specifically, this framework fails to account for potential radiative warming due to macroalgae-induced increases in surface albedo [30] and neglects the impact of CDR-driven reductions in atmospheric CO_2 concentrations on the terrestrial biosphere [29].

5. Conclusion

We demonstrate in idealized high-resolution ocean biogeochemical model simulations that physicochemical constraints limit the global efficiency of macroalgae CDR to an upper bound of 79% of the macroalgae carbon production rate. This CDR efficiency decreases to an upper bound of 58% when macroalgae are unfertilised and nutrient constraints on production and planktonic feedbacks are considered, indicating that failing to account for the impact of macroalgae nutrient consumption on phytoplankton production leads to an overestimation of the efficiency of macroalgae-based CDR. At regional scales, CDR efficiency is widely variable, with macroalgae production even resulting in a reduction in the ocean carbon sink in certain regions. Of the 73 million km^2 suitable for macroalgal culture in our simulations, only 0.3 million km^2 exhibit a local CDR efficiency greater than 80%, highlighting the critical choice of cultivation location. We found Eastern boundary upwelling systems and regions of the Northeast Pacific and the Southern Ocean as potentially promising regions for efficient macroalgae-based CDR. Our analysis further indicates that half of the enhanced air–sea carbon flux occurs outside macroalgae cultivation areas, potentially hindering the monitoring and verification of CDR that any real-world deployment is likely to require. Under the magnitude of macroalgae production rates considered here, we find limited potential for ocean acidification co-benefits and often substantial reductions in phytoplankton primary production which could impact wild food webs.

Data availability statement

The data that support the findings of this study are available upon reasonable request from the authors.

Acknowledgments

The authors thank the IPSL modelling group for the software infrastructure, which facilitated model simulations and analysis. Authors received funding from the EU H2020 Projects 4C (Grant No. 821003) and COMFORT (Grant 820989), and the ENS-Chanel research chair. Simulations were carried out with computational resources from TGCC through a GENCI/DARI Grant (gen0040). This study benefited from the ESPRI (Ensemble de Services Pour la Recherche l'IPSL) computing and data center (https://mesocentre.ipsl.fr) which is supported by

CNRS, Sorbonne Université, École Polytechnique, and CNES and through national and international grants.

Conflict of interest

The authors declare that they have no conflict of interests.

ORCID iDs

Manon Berger https://orcid.org/0000-0002-6519-5393
David T Ho https://orcid.org/0000-0002-0944-6952

References

[1] IPCC 2022 *Climate Change 2022: Mitigation of Climate Change. Contribution of Working Group III to the Sixth Assessment Report of the Intergovernmental Panel on Climate Change* (Cambridge: Cambridge University Press) (https://doi.org/10.1017/9781009157926)
[2] IPCC 2022 Summary for policymakers *Climate Change 2022: Mitigation of Climate Change. Contribution of Working Group III to the Sixth Assessment Report of the Intergovernmental Panel on Climate Change* (Cambridge: Cambridge University Press) (https://doi.org/10.1017/9781009157926.001)
[3] Rogelj J *et al* 2018 Scenarios towards limiting global mean temperature increase below 1.5 °C *Nat. Clim. Change* **8** 325–32
[4] IPCC (ed) 2022 Mitigation pathways compatible with 1.5 °C in the context of sustainable development *Global warming of 1.5 °C: IPCC special report on impacts of global warming of 1.5 °C above pre-industrial levels in context of strengthening response to climate change, sustainable development, and efforts to eradicate poverty* (Cambridge: Cambridge University Press) pp 93–174
[5] Minx J C, Lamb W F, Callaghan M W, Bornmann L and Fuss S 2017 Fast growing research on negative emissions *Environ. Res. Lett.* **12** 035007
[6] Kriegler E, Luderer G, Bauer N, Baumstark L, Fujimori S and Popp A 2018 Pathways limiting warming to 1.5 °C: a tale of turning around in no time? *Phil. Trans.* A **376** 20160457
[7] Pathak M, Slade R, Shukla P R, Skea J, Pichs-Madruga R and Ürge-Vorsatz D 2022 Technical summary *Climate Change 2022: Mitigation of Climate Change. Contribution of Working Group III to the Sixth Assessment Report of the Intergovernmental Panel on Climate Change* (Cambridge: Cambridge University Press) (https://doi.org/10.1017/9781009157926.002)
[8] Minx J C *et al* 2018 Negative emissions—part 1: research landscape and synthesis *Environ. Res. Lett.* **13** 063001
[9] Gattuso J-P, Magnan A K, Bopp L, Cheung W W L, Duarte C M and Hinkel J 2018 Ocean solutions to address climate change and its effects on marine ecosystems *Front. Mar. Sci.* **5** 337
[10] Boyd P W 2019 High level review of a wide range of proposed marine geoengineering techniques *Rep. Stud. GESAMP* No. 98 (GESAMP (IMO/FAO/UNESCO-IOC/UNIDO/WMO/IAEA/UN/UN Environment/ UNDP/ISA Joint Group of Experts on the Scientific Aspects of Marine Environmental Protection) p 144
[11] IPCC 2014 *Glossary. Climate Change 2014—Impacts, Adaptation and Vulnerability: Part B: Regional Aspects: Working Group II Contribution to the IPCC Fifth Assessment Report: Volume 2: Regional Aspects* vol 2 (Cambridge: Cambridge University Press) pp 1757–76
[12] Duarte C M, Wu J, Xiao X, Bruhn A and Krause-Jensen D 2017 Can seaweed farming play a role in climate change mitigation and adaptation? *Front. Mar. Sci.* **4** 100
[13] Krause-Jensen D, Lavery P, Serrano O, Marbà N, Masque P and Duarte C M 2018 Sequestration of macroalgal carbon: the elephant in the blue carbon room *Biol. Lett.* **14** 20180236
[14] Froehlich H E, Afflerbach J C, Frazier M and Halpern B S 2019 Blue growth potential to mitigate climate change through seaweed offsetting *Curr. Biol.* **29** 3087–93.e3
[15] Mann K H 1973 Seaweeds: their productivity and strategy for growth *Science* **182** 975–81
[16] Scurlock J M and Olson R J 2002 Terrestrial net primary productivity—a brief history and a new worldwide database *Environ. Rev.* **10** 91–109
[17] Fernand F, Israel A, Skjermo J, Wichard T, Timmermans K R and Golberg A 2017 Offshore macroalgae biomass for bioenergy production: environmental aspects, technological achievements and challenges *Renew. Sustain. Energy Rev.* **75** 35–45
[18] Gao G, Gao L, Jiang M, Jian A and He L 2021 The potential of seaweed cultivation to achieve carbon neutrality and mitigate deoxygenation and eutrophication *Environ. Res. Lett.* **17** 014018
[19] de N'yeurt A R, Chynoweth D P, Capron M E, Stewart J R and Hasan M A 2012 Negative carbon via ocean afforestation *Process Saf. Environ. Prot.* **90** 467–74
[20] Boyd P W, Bach L T, Hurd C L, Paine E, Raven J A and Tamsitt V 2022 Potential negative effects of ocean afforestation on offshore ecosystems *Nat. Ecol. Evol.* **6** 675–83
[21] Campbell I, Macleod A, Sahlmann C, Neves L, Funderud J and Øverland M 2019 The environmental risks associated with the development of seaweed farming in Europe—prioritizing key knowledge gaps *Front. Mar. Sci.* **6** 107
[22] Orr J C and Sarmiento J L 1992 Potential of marine macroalgae as a sink for CO_2: constraints from a 3D general circulation model of the global ocean *Water Air Soil Pollut.* **64** 405–21
[23] Howard J, Sutton-Grier A, Herr D, Kleypas J, Landis E, Mcleod E, Pidgeon E and Simpson S 2017 Clarifying the role of coastal and marine systems in climate mitigation *Front. Ecol. Environ.* **15** 42–50
[24] Gallagher J B, Shelamoff V and Layton C 2022 Seaweed ecosystems may not mitigate CO_2 emissions *ICES J. Mar. Sci.* **79** fsac011
[25] Hurd C L, Law C S, Bach L T, Britton D, Hovenden M, Paine E, Raven J A, Tamsitt V and Boyd P W 2022 Forensic carbon accounting: assessing the role of seaweeds for carbon sequestration *J. Phycol.* **58** 347–63
[26] Duarte C M, Bruhn A and Krause-Jensen D 2022 A seaweed aquaculture imperative to meet global sustainability targets *Nat. Sustain.* **5** 185–93
[27] Frieder C A, Yan C, Chamecki M, Dauhajre D, McWilliams J C and Infante J 2022 A macroalgal cultivation modeling system (MACMODS): evaluating the role of physical-biological coupling on nutrients and farm yield *Front. Mar. Sci.* **9** 214
[28] Arzeno-Soltero I, Frieder C, Saenz B, Long M, DeAngelo J and Davis S J 2022 Biophysical potential and uncertainties of global seaweed farming (https://doi.org/10.31223/X52P8Z) (Accessed 11 January 2023)
[29] Wu J, Keller D P and Oschlies A 2022 Carbon dioxide removal via macroalgae open-ocean mariculture and sinking: an earth system modeling study *Earth Syst. Dyn. Discuss.* (Accessed 11 January 2023)
[30] Bach L T, Tamsitt V, Gower J, Hurd C L, Raven J A and Boyd P W 2021 Testing the climate intervention potential of ocean afforestation using the Great Atlantic Sargassum Belt *Nat. Commun.* **12** 2556
[31] Ocean Visions (available at: www2.oceanvisions.org/roadmaps/macroalgae-cultivation-carbon-sequestration/development-gaps-and-needs/) (Accessed 12 November 2022)

[32] Fichefet T and Maqueda M A M 1997 Sensitivity of a global sea ice model to the treatment of ice thermodynamics and dynamics *J. Geophys. Res.* **102** 12609–46
[33] Aumont O, Ethé C, Tagliabue A, Bopp L and Gehlen M 2015 PISCES-v2: an ocean biogeochemical model for carbon and ecosystem studies *Geosci. Model Dev.* **8** 2465–513
[34] Barnier B *et al* 2009 Impact of partial steps and momentum advection schemes in a global ocean circulation model at eddy-permitting resolution *Ocean Dyn.* **59** 537
[35] Terhaar J, Orr J C, Gehlen M, Ethé C and Bopp L 2019 Model constraints on the anthropogenic carbon budget of the Arctic Ocean *Biogeosciences* **16** 2343–67
[36] Dussin R, Barnier B, Brodeau L and Molines J M 2016 *The Making of Drakkar Forcing Set DFS5* (LGGE)
[37] Raven J A and Hurd C L 2012 Ecophysiology of photosynthesis in macroalgae *Photosyn. Res.* **113** 105–25
[38] Cai J *et al* 2021 *Seaweeds and Microalgae: An Overview for Unlocking Their Potential in Global Aquaculture Development (FAO Fisheries and Aquaculture Circular* No. 1229) (Rome: Food and Agriculture Organization of the United Nations) p 48
[39] Breeman A M 1988 Relative importance of temperature and other factors in determining geographic boundaries of seaweeds: experimental and phenological evidence *Helgoländer Meeresuntersuchungen* **42** 199–241
[40] Harrison P and Hurd C 2001 Nutrient physiology of seaweeds: application of concepts to aquaculture *Cah. Biol. Mar.* **42** 71–82
[41] Sharma S, Neves L, Funderud J, Mydland L T, Øverland M and Horn S J 2018 Seasonal and depth variations in the chemical composition of cultivated *Saccharina latissima* *Algal Res.* **32** 107–12
[42] Zimmerman R and Kremer J 1986 *In situ* growth and chemical composition of the giant kelp, *Macrocystis pyrifera*: response to temporal changes in ambient nutrient availability *Mar. Ecol. Prog. Ser.* **27** 277–85
[43] Stewart H, Fram J, Reed D, Williams S, Brzezinski M, MacIntyre S and Gaylord B 2009 Differences in growth, morphology and tissue carbon and nitrogen of *Macrocystis pyrifera* within and at the outer edge of a giant kelp forest in California, USA *Mar. Ecol. Prog. Ser.* **375** 101–12
[44] van Tussenbroek B I 1989 Seasonal growth and composition of fronds of *Macrocystis pyrifera* in the Falkland Islands *Mar. Biol.* **100** 419–30
[45] Gevaert F, Janquin M A and Davoult D 2008 Biometrics in *Laminaria digitata*: a useful tool to assess biomass, carbon and nitrogen contents *J. Res.* **60** 215–9
[46] Ross A, Jones J, Kubacki M and Bridgeman T 2008 Classification of macroalgae as fuel and its thermochemical behaviour *Bioresour. Technol.* **99** 6494–504
[47] Schiener P, Black K D, Stanley M S and Green D H 2015 The seasonal variation in the chemical composition of the kelp species *Laminaria digitata, Laminaria hyperborea, Saccharina latissima* and *Alaria esculenta J. Appl. Phycol.* **27** 363–73
[48] Atkinson M J and Sv S 1983 C:N:P ratios of benthic marine plants1 *Limnol. Oceanogr.* **28** 568–74
[49] Duarte C M *et al* 2022 Global estimates of the extent and production of macroalgal forests *Glob. Ecol. Biogeogr.* **31** 1422–39
[50] Duarte C M 1992 Nutrient concentration of aquatic plants: patterns across species *Limnol. Oceanogr.* **37** 882–9
[51] Takahashi T, Broecker W S and Langer S 1985 Redfield ratio based on chemical data from isopycnal surfaces *J. Geophys. Res.* **90** 6907–24
[52] Jones D C, Ito T, Takano Y and Hsu W-C 2014 Spatial and seasonal variability of the air-sea equilibration timescale of carbon dioxide *Glob. Biogeochem. Cycles* **28** 1163–78
[53] Wanninkhof R, Asher W E, Ho D T, Sweeney C and McGillis W R 2009 Advances in quantifying air-sea gas exchange and environmental forcing *Ann. Rev. Mar. Sci.* **1** 213–44
[54] Wanninkhof R 1992 Relationship between wind speed and gas exchange over the ocean *J. Geophys. Res.* **97** 7373–82
[55] Weiss R F 1974 Carbon dioxide in water and seawater: the solubility of a non-ideal gas *Mar. Chem.* **2** 203–15
[56] Egleston E S, Sabine C L and Morel F M M 2010 Revelle revisited: buffer factors that quantify the response of ocean chemistry to changes in DIC and alkalinity *Glob. Biogeochem. Cycles* **24**
[57] Hein M, Pedersen M F and Sand-Jensen K 1995 Size-dependent nitrogen uptake in micro- and macroalgae *Mar. Ecol. Prog. Ser.* **118** 247–53